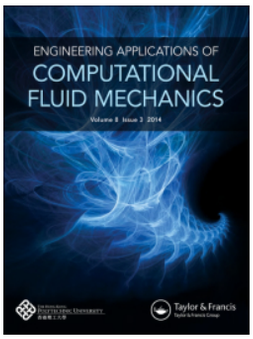

Taylor & Francis
Taylor & Francis Group

Engineering Applications of Computational Fluid Mechanics

ISSN: (Print) (Online) Journal homepage: https://www.tandfonline.com/loi/tcfm20

Energetic thermo-physical analysis of MLP-RBF feed-forward neural network compared with RLS Fuzzy to predict CuO/liquid paraffin mixture properties

Xiaoluan Zhang, Xinni Liu, Xifeng Wang, Shahab S. Band, Seyed Amin Bagherzadeh, Somaye Taherifar, Ali Abdollahi, Mehrdad Bahrami, Arash Karimipour, Kwok-Wing Chau & Amir Mosavi

To cite this article: Xiaoluan Zhang, Xinni Liu, Xifeng Wang, Shahab S. Band, Seyed Amin Bagherzadeh, Somaye Taherifar, Ali Abdollahi, Mehrdad Bahrami, Arash Karimipour, Kwok-Wing Chau & Amir Mosavi (2022) Energetic thermo-physical analysis of MLP-RBF feed-forward neural network compared with RLS Fuzzy to predict CuO/liquid paraffin mixture properties, Engineering Applications of Computational Fluid Mechanics, 16:1, 764-779, DOI: 10.1080/19942060.2022.2046167

To link to this article: https://doi.org/10.1080/19942060.2022.2046167

Published online: 14 Mar 2022.

ENGINEERING APPLICATIONS OF COMPUTATIONAL FLUID MECHANICS
2022, VOL. 16, NO. 1, 764–779
https://doi.org/10.1080/19942060.2022.2046167

Taylor & Francis
Taylor & Francis Group

Energetic thermo-physical analysis of MLP-RBF feed-forward neural network compared with RLS Fuzzy to predict CuO/liquid paraffin mixture properties

Xiaoluan Zhang[a], Xinni Liu[b], Xifeng Wang[a], Shahab S. Band[c], Seyed Amin Bagherzadeh[d], Somaye Taherifar[e], Ali Abdollahi[d], Mehrdad Bahrami[d], Arash Karimipour[d], Kwok-Wing Chau [f] and Amir Mosavi [g,h,i]

[a]School of Computer Sciences, Baoji University of Arts and Sciences, Baoji, People's Republic of China; [b]School of Information, Xi'an University of Finance and Economics, Xi'an, People's Republic of China; [c]Future Technology Research Center, College of Future, National Yunlin University of Science and Technology, Douliou, Taiwan; [d]Department of Mechanical Engineering, Najafabad Branch, Islamic Azad University, Najafabad, Iran; [e]Department of Computer Sciences, Faculty of Mathematical Sciences and Computer, Shahid Chamran University of Ahvaz, Ahavaz, Iran; [f]Department of Civil and Environmental Engineering, Hong Kong Polytechnic University, Hong Kong, People's Republic of China; [g]John von Neumann Faculty of Informatics, Obuda University, Budapest, Hungary; [h]Institute of Information Engineering, Automation and Mathematics, Slovak University of Technology in Bratislava, Bratislava, Slovakia; [i]Institute of Information Society, University of Public Service, Budapest, Hungary

ABSTRACT

Dynamic viscosity of novel generated Copper Oxide (CuO)/Liquid Paraffin nanofluids is obtained experimentally for various temperatures and concentrations. To optimize the empirical process and for cost-efficiency, Feed-Forward Neural Networks (FFNNs) were modeled and compared with Recursive Least Squares (RLS) Fuzzy model. To prepare CuO/ liquid paraffin nanofluids, CuO nanoparticles are dispersed within paraffin. Then an input-target dataset containing 30 input-target pairs is available for $T = 25, 35, 40, 50, 55, 70(^{\circ}C)$, and $\varphi = 0.1,\ 0.5,\ 1.0\ ,\ 3.0,\ 5.0$ (%). Based on the empirical results, two types of FFNNs are examined and compared with RLSF model to predict CuO/liquid paraffin nanofluids. To evaluate the best optimization methods of nanofluid viscosity, Multi-Layer Feed forward (MLF), Radial Basis Function (RBF), and RLSF are compared and discussed. The MLF network provides a global approximation while the RBF acts more locally, further, RLSF provides a better fit. On the contrary, the RBF network has better properties from the generalization and noise rejection points of view. Also, RBF networks can be applied in an online manner. Further, three curves of RLS Fuzzy model by Parabola2D, ExtremeCum, and Poly2D models were fitted on the empirical data and compared. The ExtremeCum model showed the least margin of error and can be employed to predict the data.

ARTICLE HISTORY
Received 25 August 2020
Accepted 19 February 2022

KEYWORDS
Viscosity; copper oxide; liquid paraffin; artificial intelligence; RLS Fuzzy; machine learning

1. Introduction

One of the main incentives for the application of nanofluids in the industry is the thermal conductivity of the nanoparticles, which results in increased heat transfer. It causes a significant improvement in the conduction of the mixture. However, nanoparticles Brownian motions can cause the activation of the nanofluid convention. Besides, because of the hybrid nanoparticles' lower concentration, the costs are reduced, and the efficiency is increased. Additionally, different kinds of base liquids can be studied depending on the operational conditions (Abdalla et al., 2010; Rajpal, 2014; Santos et al., 2013). Hence, it seems necessary that one should have an acceptable level of knowledge regarding nanofluid thermophysical properties, particularly for the new kinds of nanofluid. The heat transfer rate and thermal efficiency are among the advantages of encouraging applying the nanofluid. Various studies have reported these advantages. Because of the high-cost empirical works on nanofluid, some studies have utilized numerical approaches. A correlation is proposed in these works. It is between the favorite subjects of researchers in the field of composites and nanofluids (Akhlaghi & Kompany-Zareh, 2005; Bagwari et al., 2015; Ghasemi & Karimipour, 2018). The experimental studies have some problems, and some specific matters should be taken into account. Hence, it is suggested to use the numerical approaches to predict fluid properties at the optimal condition. Generally, the ANN method is utilized for estimating the thermo-physical characteristics according to the empirical data. Because of the universal approximation property of the ANN approach, it is considered the most leading regression approach.

CONTACT Xifeng Wang dweisky@yeah.net; Shahab S. Band shamshirbands@yuntech.edu.tw

A multi-layer feed-forward can anticipate the relationships between the independent and dependent variables. Among the optimization methods, the artificial neural network (ANN) has been applied in numerous studies for predicting the nanofluid characteristics, particularly for its viscosity and thermal conductivity. Besides, the acceptable accuracy of this approach motivates the researchers to construct newer ANN models for better consistency with the available physical conditions of a nanofluid flow (Abdollahi et al., 2018; Dehghani et al., 2019; Karimipour et al., 2018; Sedeh et al., 2019; Teng et al., 2010).

Current progress in machine learning (ML) suggests novel tools to excerpt novel understandings from large data sets and to achieve small data sets more efficiently (Ahmadi, Ahmadi et al., 2014; Ali Ahmadi & Ahmadi, 2016; Amedi et al., 2016; Moosavi et al., 2019). Scientists in nanoscience are investigating with these tools to tackle demands in many fields. Further, ML's progress of nanoscience, nanoscience supports the foundation for neuromorphic computing hardware to develop the implementation of ML algorithms: (i) employing ML to analyze and extract novel understandings from large nanoscience data sets, (ii) employing ML to advance material discovery, containing the use of active learning to guide empirical design, and (iii) the nanoscience of memristive devices to realize hardware tailored for ML (Ahmadi, Ebadi, Marghmaleki et al., 2014, Ahmadi, Ebadi, & Yazdanpanah, 2014; Ahmadi, Bahadori et al., 2015; Ahmadi, Pouladi et al., 2015; Nguyen, Ghorbani et al., 2020; Shafiei et al., 2014).

Cost efficiency is the act of saving money by optimizing a process. This is done by decreasing experimental costs and improving efficiencies across the process (Abidi et al., 2021; Du et al., 2020; Nguyen, Rizvandi et al., 2020; Sun et al., 2021). Liu et al. (2019) presented a new approach of 'Recursive Least Squares Fuzzy' neural network. They optimized the thermal conductivity measurement of Graphene Oxide/Water nanofluid by *R*-Squared of 0.99. Alsarraf, Malekahmadi et al. (2020) used the neural network to optimized the thermal conductivity measurement of Graphene/Water nanofluid by *R*-Squared of 0.99. Xu et al. (2020) used Levenberg Marquardt (LM) algorithm to optimize the viscosity measurement process of Graphene Oxide/Water nanofluid by *R*-Squared of 0.997 for RMPs of 10 and 100. Li et al. (2021) presented a novel neural network algorithm (Orthogonal Distance Regression (ODR)) to optimize the thermal conductivity measurement of Carbon Nanotube-Titanium Dioxide/Water-Ethylene Glycol nanofluid by *R*-Squared of 0.9999. Malekahmadi et al. (2021) compared two kinds of neural network algorithms, LM and ODR, to find the best optimization method for thermal conductivity measurement of Carbon Nanotube-Hydroxyapatite/Water nanofluid. They reported that the ODR is a better method to model the process and to reduce the cost of experiments.

For neural networks models, Ebtehaj et al. (2018) by hybrid decision tree (DT) technique with multilayer perceptron (MLP) and radial basis function (RBF) artificial neural networks, indicated that it is possible to extract matrices to provide applicable models. Also, Ebtehaj and Bonakdari (2016) optimized Multilayer Perceptron (MLP) network with three different training algorithms, including variable learning rate (MLP-GDX), resilient back-propagation (MLP-RP) and Levenberg-Marquardt (MLPLM) to apply in the practical application.

ANN optimization method is examined based on empirical data of the CuO/ liquid paraffin nanofluids in volume fraction 0.1, 0.5, 1.0, 3.0 and 5.0, and in the temperature range 25–70°C. To evaluate the best optimization method of nanofluid viscosity, MLF, RBF and RLS Fuzzy are compared and discussed (Al-Rashed et al., 2019; Alsarraf, Shahsavae et al., 2020a; Izadi et al., 2018; Jiang et al., 2019; Ranjbarzadeh et al., 2017, 2018, 2019; Safaei et al., 2019).

2. Numerical method

Artificial Neural Networks (ANNs) are frequently used for curve fitting and function estimation. The ANNs are very successful in this regard due to their iterative process, by which the precision of the outputs is continuously improved. Since the ANNs have nonlinear activation functions, they can approximate any arbitrary function without knowing the investigated data. Despite effective applications of the ANN in the curve fitting and function approximation fields, it is not easy to select the proper type of ANNs in practice. In this paper, two types of Feed-Forward Neural Networks (FFNNs) are examined and compared with RLS Fuzzy model to predict CuO/liquid paraffin nanofluids.

Multi-Layer Perceptrons (MLPs) are the most popular type of FFNNs for curve fitting, pattern recognition, and clustering. In this method, any neuron in a specified layer collects weighted outputs of all the neurons in the previous layer. The MLP networks usually have one or two hidden layers and one output layer. In any layer, the summation of the weighted inputs is mapped by an activation function to the output space. The MLP networks usually have 'sigmoid' and 'linear' neurons. Once the outputs of the networks are obtained, they can be compared with the targets. One can use a training algorithm to minimize the Mean Squared Error (MSE) between the outputs and targets. There are a variety of back-propagation training algorithms with dissimilar schemes and characteristics.

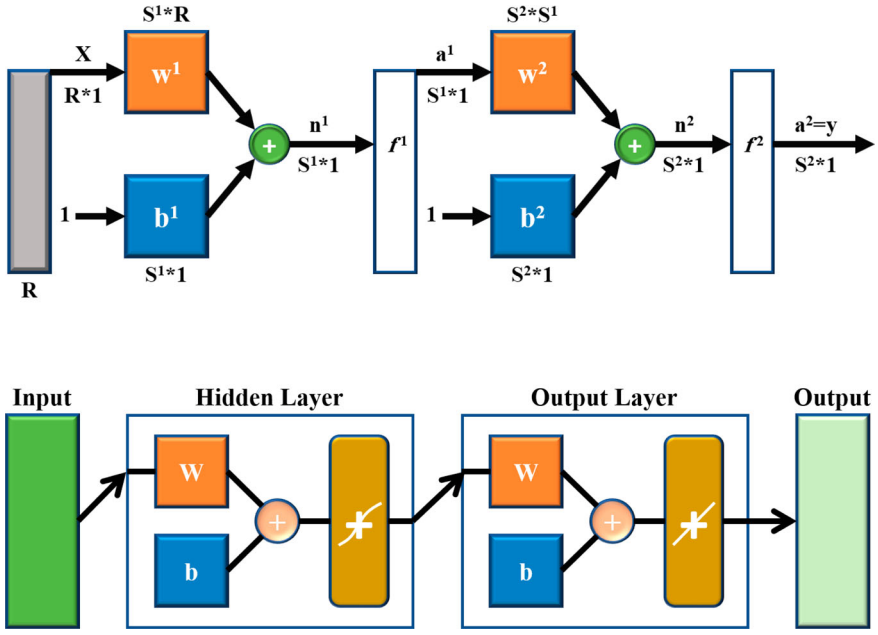

Figure 1. The architecture of two-layer MLP networks.

The MLP neuron can be mathematically described as follows:

$$y = \text{sigmoid}(w^T x + b) \tag{1}$$

in which x and y are the input and output, respectively. Also, w and b indicate the network weight and bias, respectively. Also, the 'sigmoid' activation function can be represented as follows:

$$a = \text{sigmoid}(n) = \frac{2}{1 + \exp(-2n)} - 1 \tag{2}$$

A Radial Basis Function (RBF) network consists of only one hidden layer and one output layer. The hidden layer of the RBF networks is different from the MLP ones. In the hidden layer, the Euclidean distance between the weight and input vectors are obtained. Therefore, the number of inputs and weights of the hidden layer are identical. Then, the output of the previous step is multiplied by the bias value. Finally, the net value is mapped by an activation function to the output space. The RBF network usually employs 'radbas' and 'linear' transfer functions. The training algorithm of the RBF is different from that of the MLP. The training is usually performed in a two-phase process where the centers and scaling parameters of the RBF layer are fixed in the first step, and the weights of the output layer are fixed in the second step. The RBF neuron can be mathematically described as follows:

$$y = \text{radbas}(||w - x||b) \tag{3}$$

Also, the 'radbas' activation function can be represented as follows:

$$a = \text{radbas}(n) = \exp(-n^2) \tag{4}$$

The architecture of two-layer MLP and RBF networks are illustrated schematically in Figures 1 and 2. In these figures, the first activation functions f^1 represent the 'sigmoid' and 'radbas' for the MLP and RBF networks, respectively. Also, the second activation functions f^2 are 'linear' for both cases. Also, Figure 3 is illustrated the RLS Fuzzy architecture that Layer 1 is the inputs, Layer 2 is the 'IF part', Layer 3 is the 'Rules + Norm', Layer 4 is 'THEN part', and Layer 5 is the output.

It can be observed that the MLP has simpler architecture. The MLP is widely used for diverse types of problems, while the RBF is less popular. Also, there are essential differences between the performances of the MLP and RBF networks. According to (Santos et al., 2013), the MLP network provides a global approximation while the RBF acts more locally. On the contrary, the RBF network has better properties from the generalization and noise rejection points of view. Also, RBF networks can be applied in an online manner. Due to these properties, it is not theoretically possible to select the network having the best performance. Hence, for any specific real problem, the performance of the MLP and RBF should be numerically compared (Abdalla et al., 2010; Akhlaghi & Kompany-Zareh, 2005; Bagwari et al., 2015; Rajpal, 2014; Santos et al., 2013). In this study, the performance of the

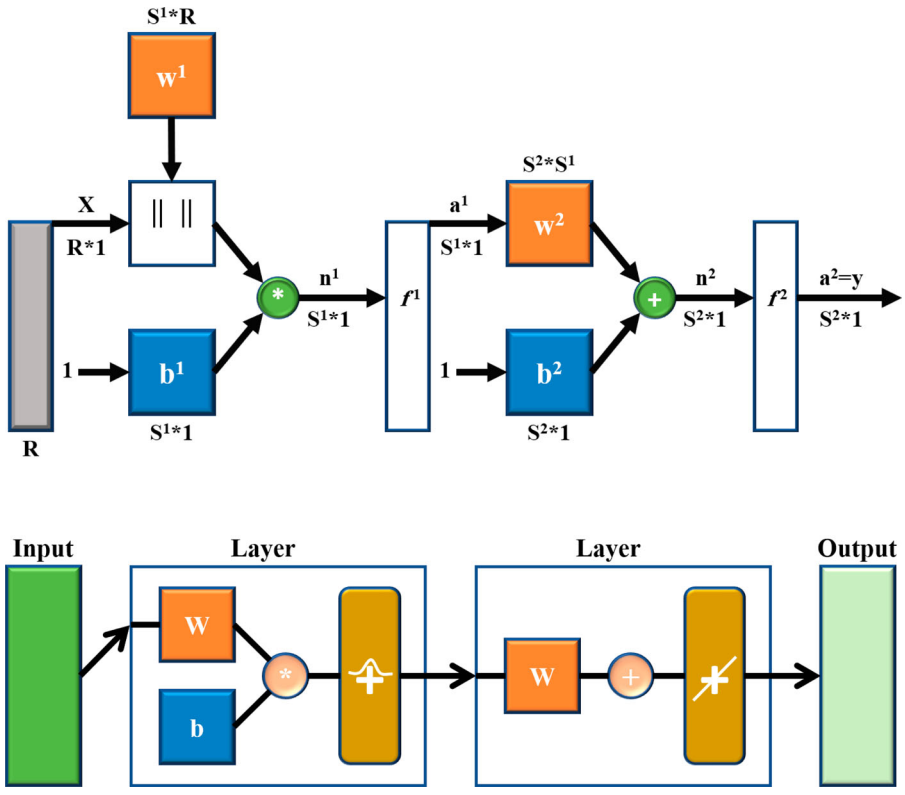

Figure 2. The architecture of two-layer RBF networks.

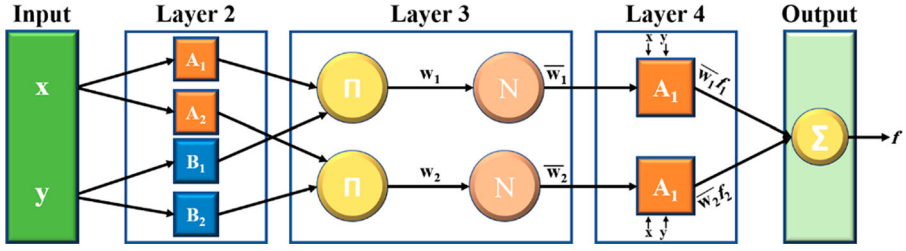

Figure 3. The architecture of RLS Fuzzy networks.

MLP, RBF and RLS Fuzzy are compared for the problem of prediction CuO/ liquid paraffin nanofluids.

Data points selection, that used to train the models, depends both on the complexity of the problem (the unknown underlying function that best relates the input variables to the output variable) and on the complexity of chosen algorithm (the algorithm used to inductively learn the unknown underlying mapping function from specific examples). Thus, the number of data points are selected based on previous related studies which are at least 30 data points to train the model (Alsarraf et al., 2020b; Liu et al., 2019; Xu et al., 2020).

The parameters of ANN, RBF, and RLSF are the learning algorithm, number of hidden layers and neurons in the hidden layer. The selection of each parameter was based on the following:

For the learning algorithm, the selection was based on the size of the training data (which is 30 in this study), Accuracy and/or Interpretability of the output (Linear Regression could easily be understood how any individual predictor is associated with the response while the flexible models give higher accuracy at the cost of low interpretability), Speed or Training time (Higher accuracy typically means higher training time, however, the training time was not an important issue in this study), Linearity (not always is the data is linear, so other algorithms are required which can handle high dimensional and complex data structures), and Number of features

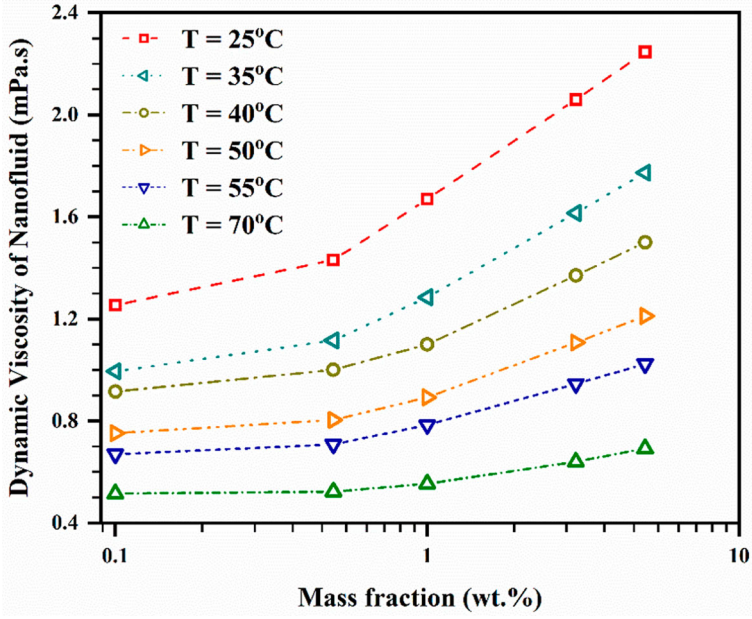

Figure 4. Value of nanofluid's dynamic viscosity at different nanoparticles mass fraction and temperature (Abdollahi et al., 2018; Dehghani et al., 2019; Ghasemi & Karimipour, 2018; Karimipour et al., 2018; Sedeh et al., 2019).

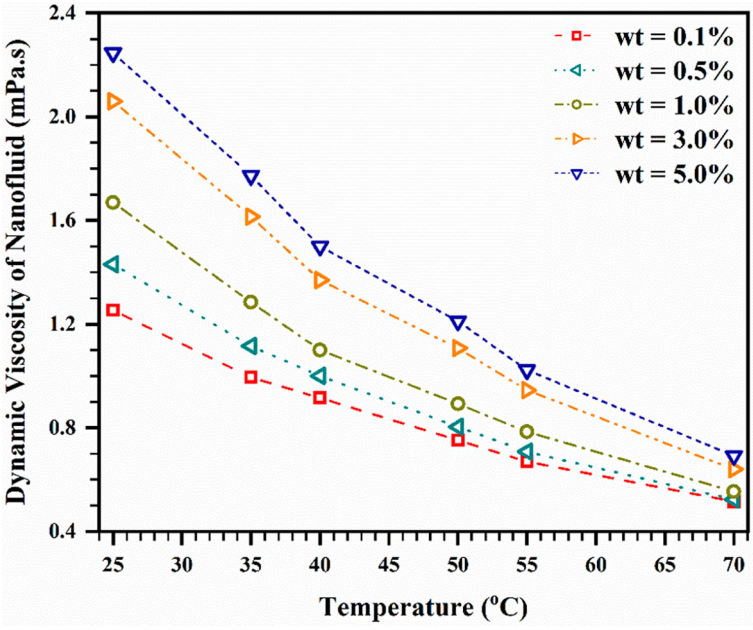

Figure 5. Experimental dynamic viscosity for various temperatures and concentrations.

(The dataset may have a large number of features that may not all be relevant and significant, however, all the datasets in this study are significant).

For the number of inputs, with respect to the number of neurons comprising this layer, this parameter is completely and uniquely determined once the shape of training data is determined. Thus, the inputs are 30 datasets. Like the Input layer, every NN has exactly one output layer. Determining its size (number of neurons) is completely determined by the chosen model configuration.

While for the hidden layers, one hidden layer is sufficient for the large majority of problems. However, the optimal size of the hidden layer is usually between the size of the input and size of the output layers. To trim

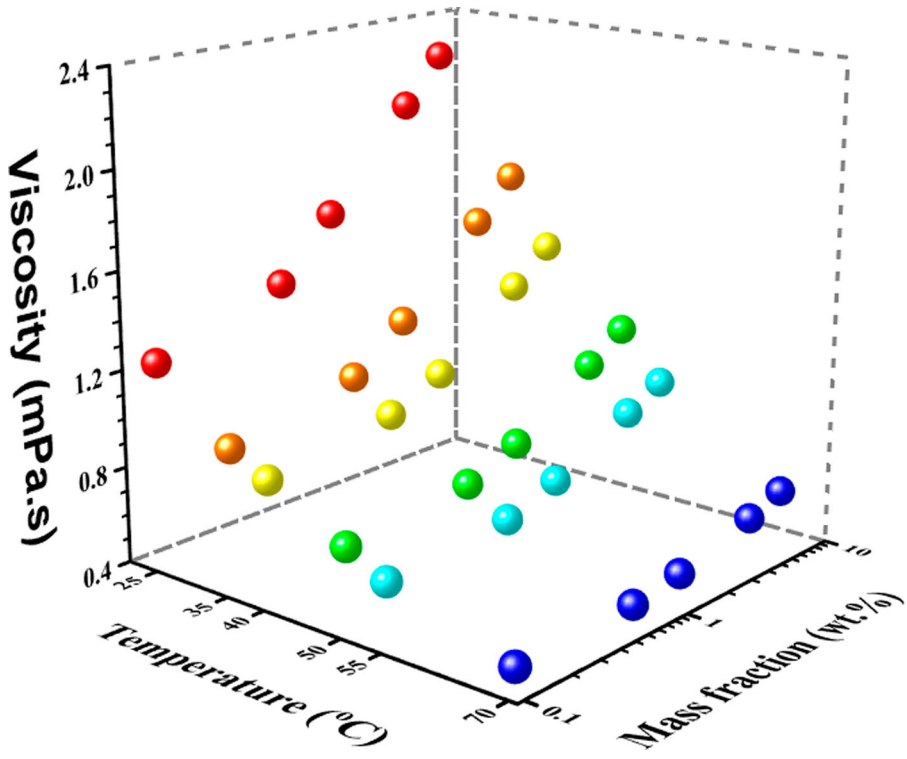

Figure 6. The experimental dynamic viscosity in semi-log axes.

network size (by nodes not layers) to improve computational performance and sometimes resolution performance, is removing nodes from the network during training by identifying those nodes which, if removed from the network, would not noticeably affect network performance (weights very close to zero in the trained matrix).

For the neurons in the hidden layer, the selection was based on the following equation which usually prevent over-fitting:

$$N_h = \frac{N_s}{(\alpha^*(N_i + N_0))} \tag{5}$$

While N_i is the number of input neurons, N_o is the number of output neurons, N_s is the number of samples in training data set, and α is an arbitrary scaling factor usually 2–10.

3. Experimentation

3.1. Materials

To prepare CuO/liquid paraffin nanofluids, CuO nanoparticles are dispersed within paraffin. All nanomaterial were obtained with the pureness of 99.91%. Furthermore, paraffin with large pureness was acquired from Merck Company, Germany. To obtain standard clean conditions, deionized water was applied to clean Entirely glaswares of the laboratory (Ghasemi & Karimipour, 2018).

3.2. Instruments

According to our previous research (Sedeh et al., 2019), Brookfield viscometer, (model DV2T, USA) is applied to measure the viscosity of the abovementioned nanofluid. Our previous study presented the morphology and sizes of dry CuO nanoparticles. Besides, a high degree of nanofluid stability is measured and confirmed according to DLS and Zeta Potential analysis (Sedeh et al., 2019). The isothermal circulator bath is applied to maintain nanofluid temperature in a certain value (Hemmat Esfe & Afrand, 2020a, 2020b; Hemmat Esfe et al., 2020; Irandoost Shahrestani et al., 2020; Khanmohammadi et al., 2020; Komeilibirjandi et al., 2020; Ma et al., 2020; Maleki et al., 2021; Rahmat et al., 2017, 2019; Wang et al., 2020; Zheng et al., 2020).

3.3. Nanofluid preparation

As mentioned in our previous research (Dehghani et al., 2019), stirring is used with 500 rpm for about 30 min to disperse 1 g of CuO nanoparticles within 19 g of paraffin. To avoid nanoparticles accumulation, the sonication waves with a maximum amplitude of 60% for three separate steps of 20 min is applied to suspension (Dehghani

et al., 2019). The specific amount of stock nanofluid was applied. In the next step, to obtain the total mass of nanofluid to reach 20 g, the paraffin was applied to the nanofluid.

4. The experimental viscosity evaluation

To assure the results, the evaluation was repeated three times in an identical situation, and deviation was evaluated by applying Equation (6) (Abdollahi et al., 2018; Karimipour et al., 2018; Sedeh et al., 2019):

$$\text{S.D.} = \sqrt{\frac{\sum_i \left(R_{\mu,i} - \overline{R_\mu}\right)^2}{n^2}} \tag{6}$$

where $R_{\mu,i}$ represents the ratio of dynamic viscosity of a fluid with nanoparticles to clean basefluid, $\overline{R_\mu}$ is average relative dynamic viscosity, and n stands for numbers of repetition, which is *three* in this work. To perform the uncertainty analysis, we determined the variation of significant parameters and the variation of thermal circulator bath accuracy the precise electric balance, and viscometer are ±0.005°C, ±0.0003 gr, and ±1%, respectively (Rajpal, 2014). Equation (7) was applied to evaluate the uncertainty of tests (Teng et al., 2010):

$$U.M. = \pm\sqrt{\left(\frac{\Delta\mu}{\mu}\right)^2 + \left(\frac{\Delta w}{w}\right)^2 + \left(\frac{\Delta T}{T}\right)^2} \tag{7}$$

According to our results, the uncertainty of the dynamic viscosity of nanofluid was approximately 8.4%.

5. Results and discussion

In the conducted experiments, the dynamic viscosity of CuO/liquid paraffin nanofluids is obtained for different temperatures and nanoparticle mass fractions. An input-target dataset containing 30 input-target pairs is available for $T = 25, 35, 40, 50, 55, 70(^\circ C)$, and $\varphi = 0.1, 0.5, 1.0, 3.0, 5.0$ (%). Figure 4 presents the impact of dynamic viscosity of CuO/paraffin. According to obtained results, viscosity significantly increases as the concentration is raised. Indeed, this is mainly due to the presence of solid particles within nanofluid. Subsequently, viscosity is enhanced. Our results also demonstrated that viscosity declines meaningfully when the temperature is increased. The micro-convection of nanoparticles in basefluid is the main reason for these phenomena. Viscosity reduces 59, 64, 67, 68 and 69% at CuO nanoparticle concentration of 0.1, 0.5, 1.0, 3.0 and 5.0 wt%; while temperature varies from 25 to 70°C. The values of the dynamic viscosity are illustrated in Figure 5. Moreover, nanofluid dynamic viscosity is shown in Figure 6.

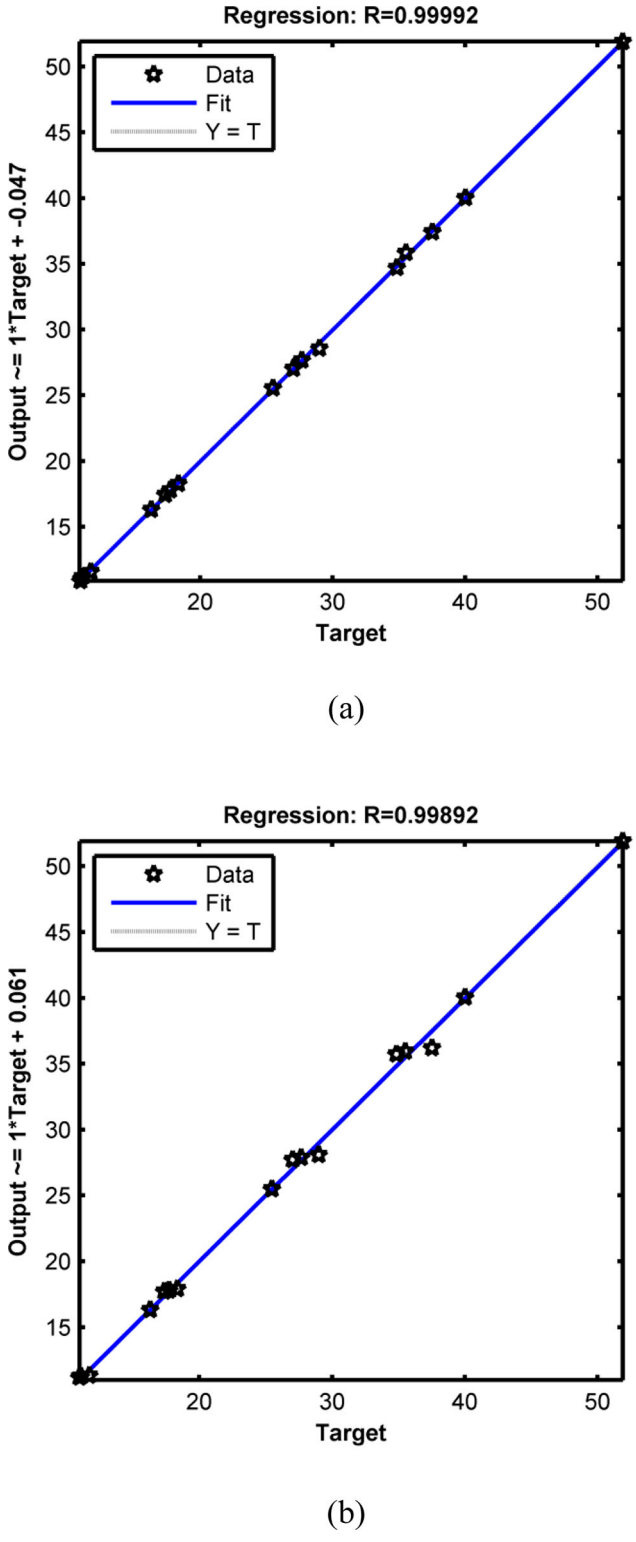

Figure 7. Experimental versus numerical data from (a) MLP, (b) RBF.

The MLP and RBF networks are applied. Regression curves are presented in Figure 7. The numerical outputs of the models are plotted against the experimental targets. It can be seen that both networks have acceptable

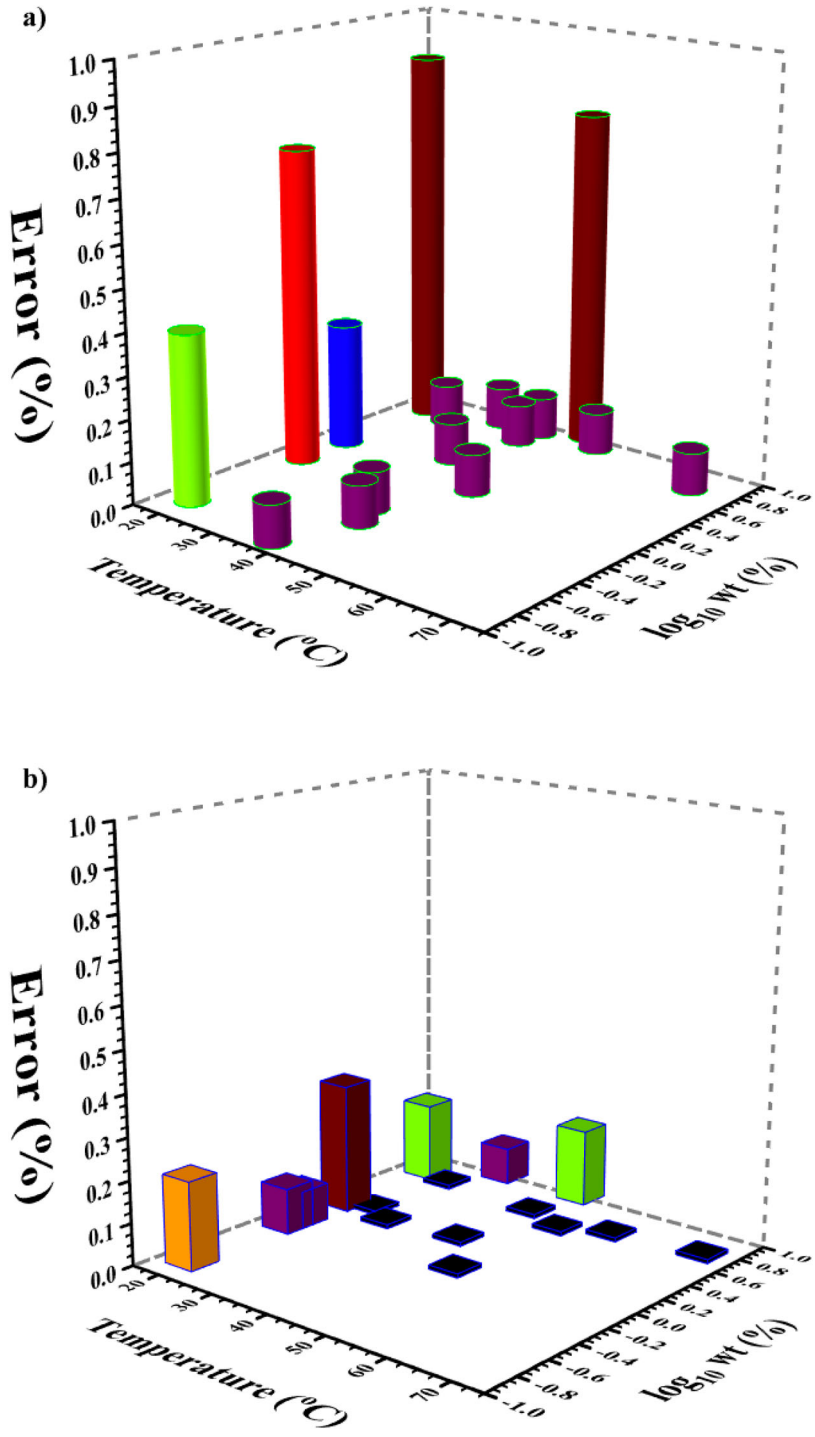

Figure 8. The error plot between experimental and numerical data by (a) MLP, (b) RBF.

performance. The error plots are shown in Figure 8(a) and (b). Results are depicted in Figure 9 for the numerical data from both methods. It can be observed that both networks result in identical predictions.

Finally, the networks are examined at non-trained inputs throughout the investigated intervals. The results are presented in Figure 10. The results of the MLP network have better smoothness. It can be concluded that the MLP network has better generalization while the RBF network has better precision. In a small training dataset, the MLP network may lead to better results, while the RBF is suggested for a large training dataset.

The RLS Fuzzy model curve fitting method applied on the empirical data based on three different models,

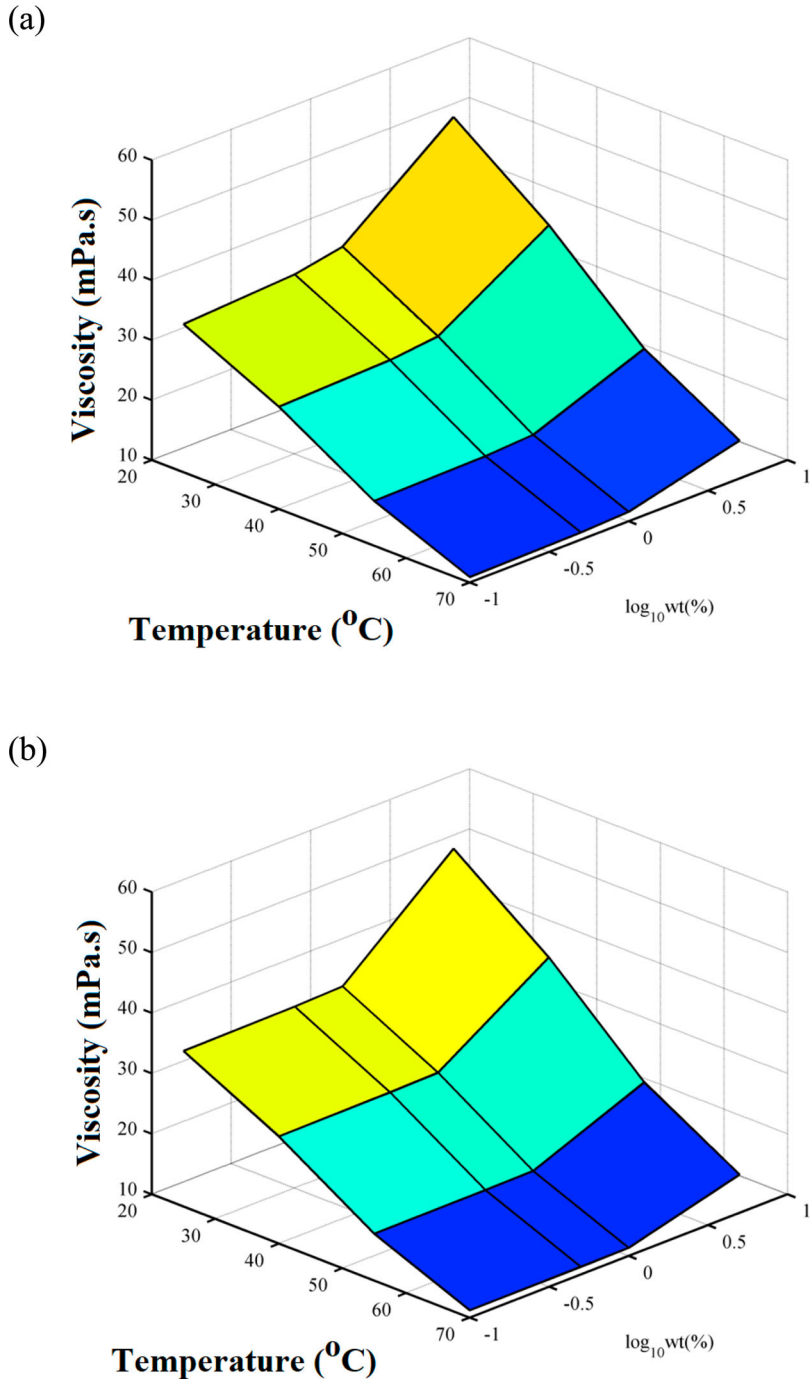

Figure 9. Numerical data by (a) MLP, (b) RBF.

'Parabola2D', 'ExtremeCum' and 'Poly2D'. As can be seen in Figure 11, Parabola2D model did not fit completely on the data, hence, ExtremeCum and Poly2D models did fit completely and can be used to predict the data.

Three original formulas derived from these three curves. As can be seen, the second Equation (ExtremeCum) has better *R*-squared (almost 1), and can be employed to predict the data.

Equation (8) is the 'Parabola2D' Eq., Equation (10) is the 'ExtremeCum' Eq., and Equation (12) is the 'Poly2D' Eq., while the Equations (9), (11), and (13) are original equations for the fitted curves of RLS Fuzzy model.

Fitted Curve: Parabola2D

$$Z = z_0 + a * X + b * Y + c * X^2 + d * Y^2 \quad (8)$$

$$\text{Viscosity} = 2.76704 + (-1.48864) * (T/T_0)$$

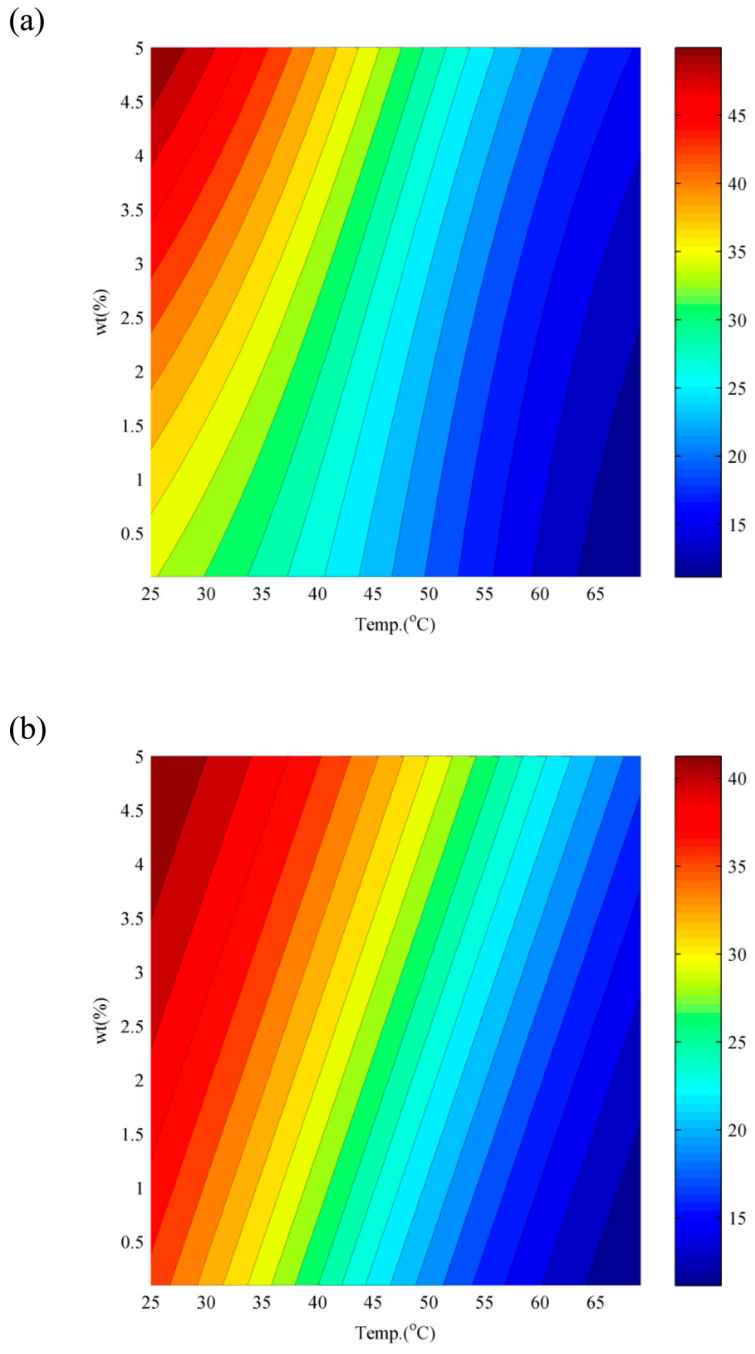

Figure 10. Numerical data by (a) MLP, (b) RBF networks at non-trained inputs throughout the investigated intervals.

$$+ 0.19591 * wt + 0.22226 * (T/T_0)^2 + (-00.1857) * wt^2 \quad (9)$$

Reduced Chi-Sqr: 0.00811, *R*-Square (COD): 0.998 43, Adj. *R*-Square: 0.99818

Fitted Curve: ExtremeCum

$$Z = z_0 + b * \exp(-\exp(-(X-c)/d)) + e * \exp(-\exp(-(Y-f)/g)) + h * \exp\left(-\exp(-(X-c)/d)\right)\left(-\exp(-(Y-f)/g)\right) \quad (10)$$

$$\text{Viscosity} = (-443.92327) + 447.23973* \exp(-\exp(-((T/T_0) - (-3.53698))/ 1.50106)) + 495.17655* \exp(-\exp(-(\text{wt} - (-6.51497))/ 2.32232)) + (-498.52483)*$$

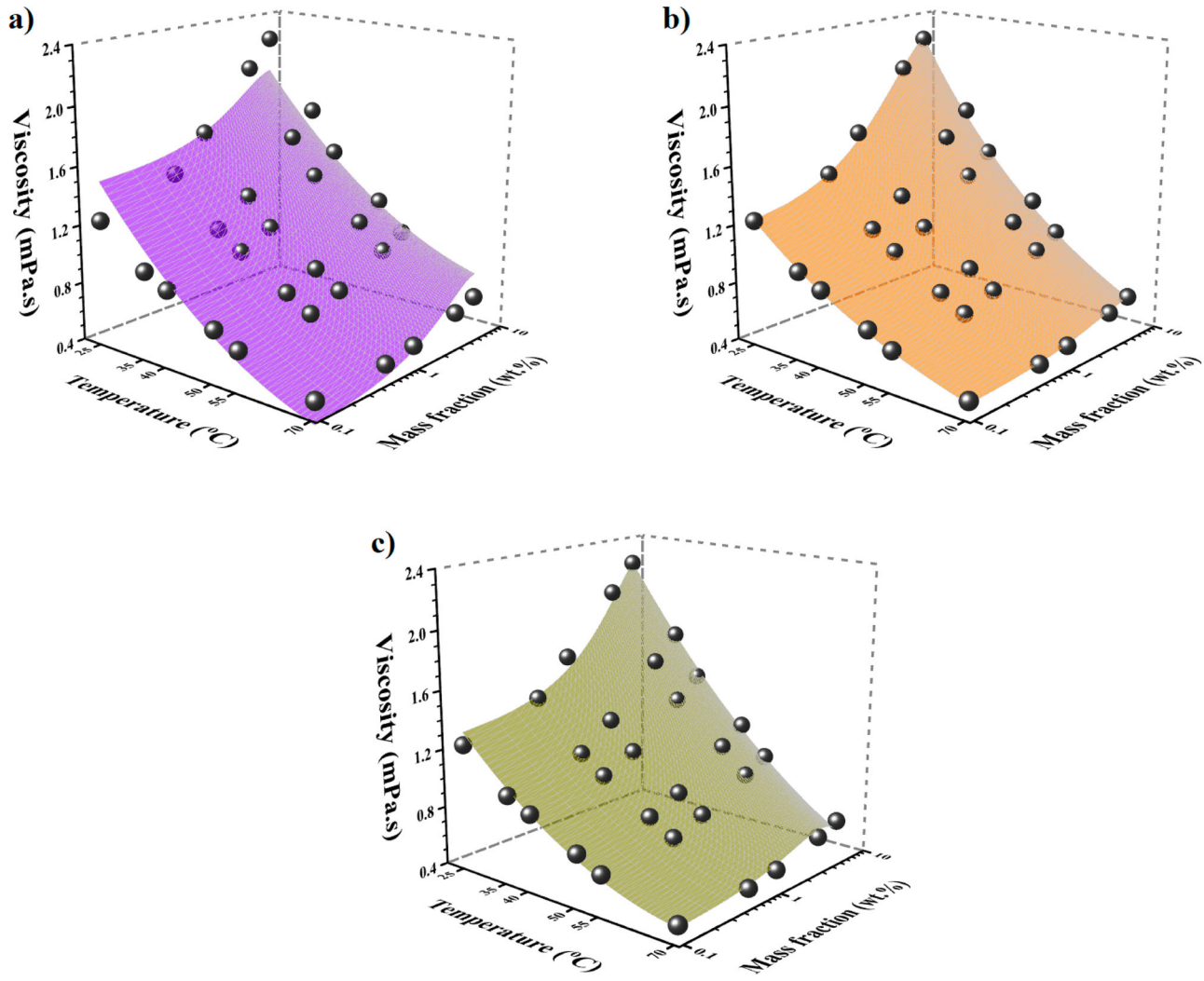

Figure 11. RLS Fuzzy model fitted curve on the empirical data by (a) Parabola2D, (b) ExtremeCum, and (c) Poly2D.

$$\exp\begin{pmatrix} -\exp(-((\mathrm{T}/\mathrm{T}_0) \\ -(-3.53698))/\ 1.50106) \\ -\exp(-(\mathrm{wt}\ -\ (-6.51497))/ \\ 2.32232) \end{pmatrix} \quad (11)$$

Reduced Chi-Sqr: 5.28744E-4, *R*-Square (COD): 0.998, Adj. *R*-Square: 0.99736

Fitted Curve: Poly2D

$$Z = z_0 + a * X + b * Y + c * X^2 + d * Y^2 + f * X * Y \quad (12)$$

$$\begin{aligned} \text{Viscosity} = {} & 2.33617 + (-1.22617) * (T/T_0) \\ & + 0.3781 * wt + 0.20149* \\ & (T/T_0)^2 + (-0.02037) * wt^2 \\ & + (-0.08835) * (T/T_0) * wt \end{aligned} \quad (13)$$

Reduced Chi-Sqr: 0.0019, *R*-Square (COD): 0.992 16, Adj. *R*-Square: 0.99053

While the T_0 is 25°C and T is the Temperature from 25 to 70°C.

Figure 12 shows Margin of error by RLS Fuzzy model. As can be seen, the Parabola2D model's error is 53.73918377% from Max. error of 23.74028975% to Min. error of −29.99889402%. The ExtremeCum model's error is 6.62089424% from Max. error of 2.656876933% to Min. error of −3.964017307%. The Poly2D model's error is 17.47650685% from Max. error of 8.032125% to Min. error of −9.444381852%. Thus, ExtremeCum model has the least margin of error and can be applied as the best fit.

Figure 13 shows the Error contour by RLS Fuzzy model. As can be seen, the dash lines are the empirical datasets while the solid lines are the trained datasets. The

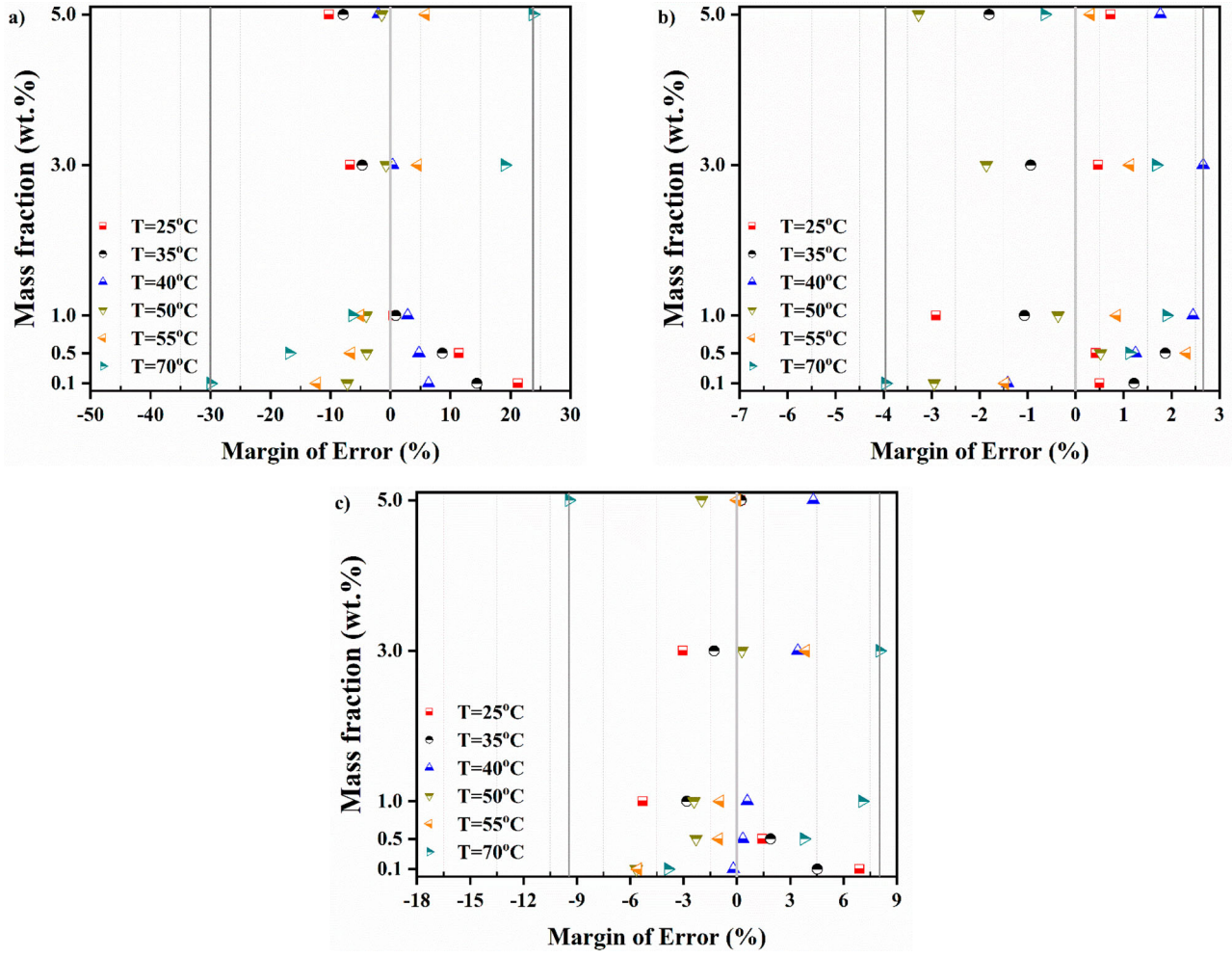

Figure 12. Margin of error by 'Recursive Least Squares Fuzzy' model for (a) Parabola2D, (b) ExtremeCum, and (c) Poly2D.

results showed that the ExtremeCum model have better smoothness.

6. Conclusion

Through the present work, the dynamic viscosity of novel generated CuO/ liquid paraffin nanofluids was obtained experimentally for various temperatures and concentrations. To prepare CuO/ liquid paraffin nanofluids, CuO nanoparticles were dispersed within paraffin. Two types of Feed-Forward Neural Networks (FFNNs) were examined and compared with RLS Fuzzy model to predict CuO/ liquid paraffin nanofluids. It was seen that the ANN optimization approach was examined based on the empirical data of CuO/ liquid paraffin nanofluids. To evaluate the best optimization method of nanofluid viscosity, MLF, RBF, and RLSF were compared and discussed. MLP network provided a global approximation while the RBF acted more locally. On the contrary, the RBF network had better properties from the generalization and noise rejection points of view. Also, RBF networks could be applied in an online manner. Moreover, the results of the MLP network had better smoothness, so the MLP network showed better generalization while RBF had better precision. Further, three curves of RLS Fuzzy model by Parabola2D, ExtremeCum, and Poly2D models were fitted on the empirical data and compared. The margin of error for Parabola2D was 53.73918%, for ExtremeCum was 6.62089%, and for Poly2D was 17.47651%. Thus, The ExtremeCum model showed the least margin of error and can be employed to predict the data.

Employing of the trained models in the case studies is possible by hybrid decision tree (DT). The viscosity measurement and its optimization by ANN and Fuzzy models can be used in a wide variety of applications within many different industries, including: Pharmaceuticals (suspensions, gelatins, and syrups); Construction industry materials (cement, coatings, and mortars); Chemicals (paints,

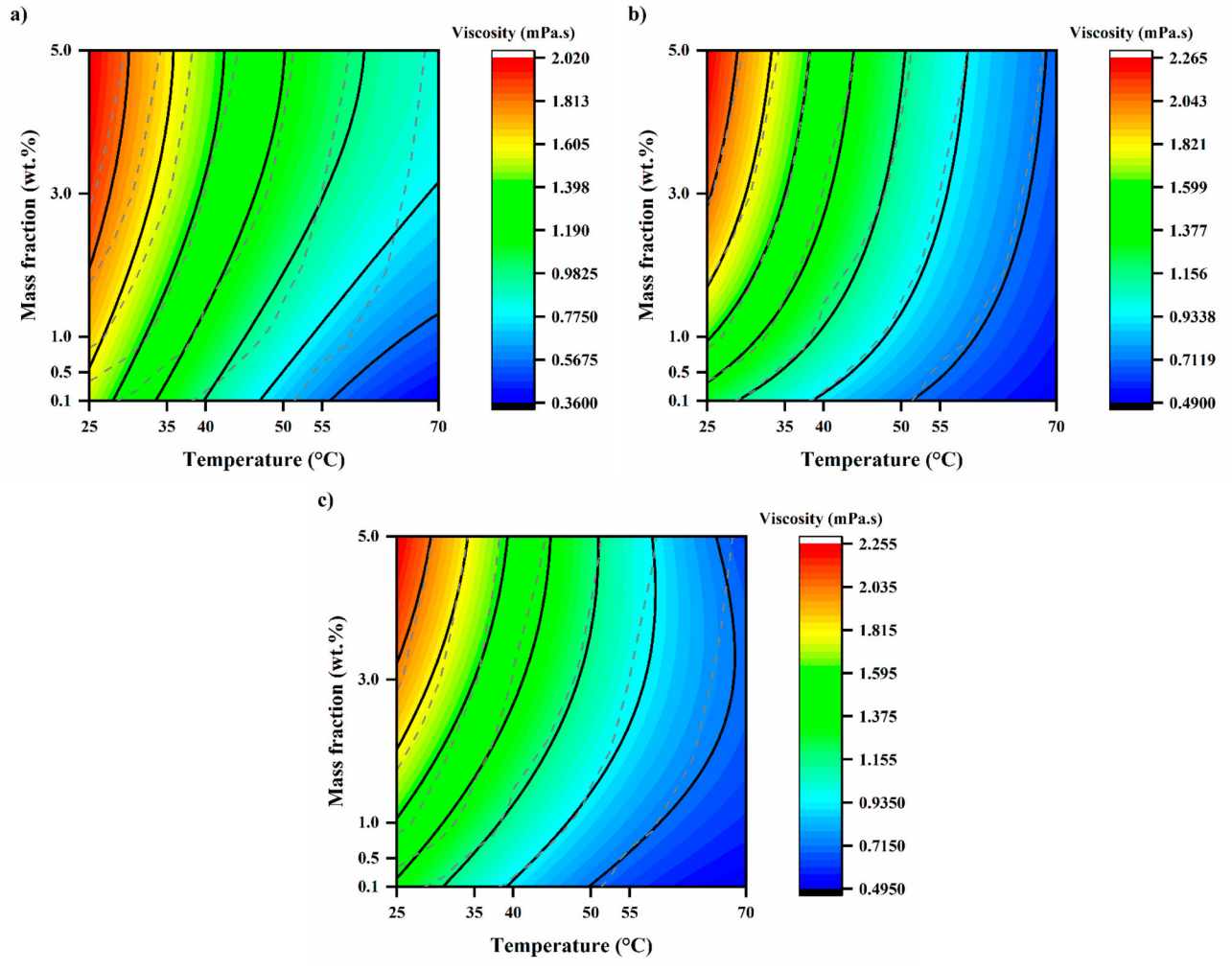

Figure 13. Error contour by 'Recursive Least Squares Fuzzy' model for (a) Parabola2D, (b) ExtremeCum, and (c) Poly2D.

inks, detergents, adhesives, and resins); and also, Foods containing seaweed, starches, soups, sauces, etc.

Disclosure statement

No potential conflict of interest was reported by the author(s).

Funding

This work was supported by Natural Science Basic Research Project of Shaanxi Province [grant number 2021JQ-765].

ORCID

Kwok-Wing Chau http://orcid.org/0000-0001-6457-161X
Amir Mosavi http://orcid.org/0000-0003-4842-0613

References

Abdalla, O. A., Zakaria, M. N., Sulaiman, S., & Ahmad, W. F. W. (2010, June). A comparison of feed-forward back-propagation and radial basis artificial neural networks: A Monte Carlo study. In *2010 international symposium on information technology* (pp. 994–998). IEEE. https://doi.org/10.1109/ITSIM.2010.5561599.

Abdollahi, A., Karimi Darvanjooghi, M. H., Karimipour, A., & Safaei, M. R. (2018). Experimental study to obtain the viscosity of CuO-loaded nanofluid: Effects of nanoparticles' mass fraction, temperature and basefluid's types to develop a correlation. *Meccanica*, *53*(15), 3739–3757. https://doi.org/10.1007/s11012-018-0916-1

Abidi, A., Jokar, Z., Allahyari, S., Sadigh, F. K., Sajadi, S. M., Firouzi, P., & Karimipour, A. (2021). Improve thermal performance of simulated-body-fluid as a solution with an ion concentration close to human blood plasma, by additive zinc oxide and its composites: ZnO/carbon nanotube and ZnO/hydroxyapatite. *Journal of Molecular Liquids*, *342*, 117457. https://doi.org/10.1016/j.molliq.2021.117457

Ahmadi, M. A., Ahmadi, M. R., Hosseini, S. M., & Ebadi, M. (2014). Connectionist model predicts the porosity and permeability of petroleum reservoirs by means of petro-physical logs: Application of artificial intelligence. *Journal of Petroleum Science and Engineering*, *123*, 183–200. https://doi.org/10.1016/j.petrol.2014.08.026

Ahmadi, M. A., Bahadori, A., & Shadizadeh, S. R. (2015). A rigorous model to predict the amount of dissolved calcium carbonate concentration throughout oil field brines: Side effect of pressure and temperature. *Fuel*, *139*, 154–159. https://doi.org/10.1016/j.fuel.2014.08.044

Ahmadi, M. A., Ebadi, M., Marghmaleki, P. S., & Fouladi, M. M. (2014). Evolving predictive model to determine condensate-to-gas ratio in retrograded condensate gas reservoirs. *Fuel*, *124*, 241–257. https://doi.org/10.1016/j.fuel.2014.01.073

Ahmadi, M. A., Ebadi, M., & Yazdanpanah, A. (2014). Robust intelligent tool for estimating dew point pressure in retrograded condensate gas reservoirs: Application of particle swarm optimization. *Journal of Petroleum Science and Engineering*, *123*, 7–19. https://doi.org/10.1016/j.petrol.2014.05.023

Ahmadi, M. A., Pouladi, B., Javvi, Y., Alfkhani, S., & Soleimani, R. (2015). Connectionist technique estimates H2S solubility in ionic liquids through a low parameter approach. *The Journal of Supercritical Fluids*, *97*, 81–87. https://doi.org/10.1016/j.supflu.2014.11.009

Akhlaghi, Y., & Kompany-Zareh, M. (2005). Comparing radial basis function and feed-forward neural networks assisted by linear discriminant or principal component analysis for simultaneous spectrophotometric quantification of mercury and copper. *Analytica Chimica Acta*, *537*(1–2), 331–338. https://doi.org/10.1016/j.aca.2004.12.079

Ali Ahmadi, M., & Ahmadi, A. (2016). Applying a sophisticated approach to predict CO_2 solubility in brines: Application to CO_2 sequestration. *International Journal of Low-Carbon Technologies*, *11*(3), 325–332. https://doi.org/10.1093/ijlct/ctu034

Al-Rashed, A. A., Ranjbarzadeh, R., Aghakhani, S., Soltanimehr, M., Afrand, M., & Nguyen, T. K. (2019). Entropy generation of boehmite alumina nanofluid flow through a minichannel heat exchanger considering nanoparticle shape effect. *Physica A: Statistical Mechanics and its Applications*, *521*, 724–736. https://doi.org/10.1016/j.physa.2019.01.106

Alsarraf, J., Malekahmadi, O., Karimipour, A., Tlili, I., Karimipour, A., & Ghashang, M. (2020). Increase thermal conductivity of aqueous mixture by additives graphene nanoparticles in water via an experimental/numerical study: Synthesise, characterization, conductivity measurement, and neural network modeling. *International Communications in Heat and Mass Transfer*, *118*(11), 104864. https://doi.org/10.1016/j.icheatmasstransfer.2020.104864

Alsarraf, J., Shahsavar, A., Khaki, M., Ranjbarzadeh, R., Karimipour, A., & Afrand, M. (2020). Numerical investigation on the effect of four constant temperature pipes on natural cooling of electronic heat sink by nanofluids: A multifunctional optimization. *Advanced Powder Technology*, *31*(1), 416–432. https://doi.org/10.1016/j.apt.2019.10.035

Amedi, H. R., Baghban, A., & Ahmadi, M. A. (2016). Evolving machine learning models to predict hydrogen sulfide solubility in the presence of various ionic liquids. *Journal of Molecular Liquids*, *216*, 411–422. https://doi.org/10.1016/j.molliq.2016.01.060

Bagwari, P., Saxena, B., Bagwari, S., & Pundir, S. (2015). Comparison of feed forward network and radial basis function for detecting and recognition of license plate. *International Journal of Computer Applications*, *118*(21), 21. https://doi.org/10.5120/20870-3360

Dehghani, Y., Abdollahi, A., & Karimipour, A. (2019). Experimental investigation toward obtaining a new correlation for viscosity of WO3 and Al_2O_3 nanoparticles-loaded nanofluid within aqueous and non-aqueous basefluids. *Journal of Thermal Analysis and Calorimetry*, *135*(1), 713–728. https://doi.org/10.1007/s10973-018-7394-5

Du, C., Nguyen, Q., Malekahmadi, O., Mardani, A., Jokar, Z., Babadi, E., & Bach, Q. V. (2020). Thermal conductivity enhancement of nanofluid by adding multiwalled carbon nanotubes: Characterization and numerical modeling patterns. *Mathematical Methods in the Applied Sciences*, ((4). https://doi.org/10.1002/mma.6466.

Ebtehaj, I., & Bonakdari, H. (2016). Bed load sediment transport estimation in a clean pipe using multilayer perceptron with different training algorithms. *KSCE Journal of Civil Engineering*, *20*(2), 581–589. https://doi.org/10.1007/s12205-015-0630-7

Ebtehaj, I., Bonakdari, H., & Zaji, A. H. (2018). A new hybrid decision tree method based on two artificial neural networks for predicting sediment transport in clean pipes. *Alexandria Engineering Journal*, *57*(3), 1783–1795. https://doi.org/10.1016/j.aej.2017.05.021

Ghasemi, S., & Karimipour, A. (2018). Experimental investigation of the effects of temperature and mass fraction on the dynamic viscosity of CuO-paraffin nanofluid. *Applied Thermal Engineering*, *128*, 189–197. https://doi.org/10.1016/j.applthermaleng.2017.09.021

Hemmat Esfe, M., & Afrand, M. (2020a). Predicting thermophysical properties and flow characteristics of nanofluids using intelligent methods: Focusing on ANN methods. *Journal of Thermal Analysis and Calorimetry*, *140*(2), 501–525. https://doi.org/10.1007/s10973-019-08789-2

Hemmat Esfe, M., & Afrand, M. (2020b). A review on fuel cell types and the application of nanofluid in their cooling. *Journal of Thermal Analysis and Calorimetry*, *140*(4), 1633–1654. https://doi.org/10.1007/s10973-019-08837-x

Hemmat Esfe, M., Afrand, M., & Esfandeh, S. (2020). Investigation of the effects of various parameters on the natural convection of nanofluids in various cavities exposed to magnetic fields: A comprehensive review. *Journal of Thermal Analysis and Calorimetry*, *140*(5), 2055–2075. https://doi.org/10.1007/s10973-019-08939-6

Irandoost Shahrestani, M., Maleki, A., Safdari Shadloo, M., & Tlili, I. (2020). Numerical investigation of forced convective heat transfer and performance evaluation criterion of Al_2O_3/water nanofluid flow inside an axisymmetric microchannel. *Symmetry*, *12*(1), 120. https://doi.org/10.3390/sym12010120

Izadi, F., Ranjbarzadeh, R., Kalbasi, R., & Afrand, M. (2018). A new experimental correlation for non-Newtonian behavior of COOH-DWCNTs/antifreeze nanofluid. *Physica E: Low-Dimensional Systems and Nanostructures*, *98*, 83–89. https://doi.org/10.1016/j.physe.2017.12.031

Jiang, Y., Sulgani, M. T., Ranjbarzadeh, R., Karimipour, A., & Nguyen, T. K. (2019). Hybrid GMDH-type neural network to predict fluid surface tension, shear stress, dynamic viscosity & sensitivity analysis based on empirical data of iron (II) oxide nanoparticles in light crude oil mixture. *Physica A: Statistical Mechanics and its Applications*, *526*, 120948–120960. https://doi.org/10.1016/j.physa.2019.04.184

Karimipour, A., Ghasemi, S., Darvanjooghi, M. H. K., & Abdollahi, A. (2018). A new correlation for estimating the thermal conductivity and dynamic viscosity of CuO/liquid paraffin nanofluid using neural network method. *International Communications in Heat and Mass Transfer*, *92*, 90–99. https://doi.org/10.1016/j.icheatmasstransfer.2018.02.002

Khanmohammadi, S., Rahimi, Z., Khanmohammadi, S., & Afrand, M. (2020). Triple-objective optimization of a double-tube heat exchanger with elliptic cross section in the presence TiO_2 nanofluid. *Journal of Thermal Analysis and Calorimetry*, *140*(1), 477–488. https://doi.org/10.1007/s10973-019-08744-1

Komeilibirjandi, A., Raffiee, A. H., Maleki, A., Alhuyi Nazari, M., & Safdari Shadloo, M. (2020). Thermal conductivity prediction of nanofluids containing CuO nanoparticles by using correlation and artificial neural network. *Journal of Thermal Analysis and Calorimetry*, *139*(4), 2679–2689. https://doi.org/10.1007/s10973-019-08838-w

Li, Y., Moradi, I., Kalantar, M., Babadi, E., Malekahmadi, O., & Mosavi, A. (2021). Synthesis of new dihybrid nanofluid of TiO_2/MWCNT in water–ethylene glycol to improve mixture thermal performance: Preparation, characterization, and a novel correlation via ANN based on orthogonal distance regression algorithm. *Journal of Thermal Analysis and Calorimetry*, *144*(6), 2587–2603. https://doi.org/10.1007/s10973-020-10392-9

Liu, W. I., Malekahmadi, O., Bagherzadeh, S. A., Ghashang, M., Karimipour, A., Hasani, S., & Goodarzi, M. (2019). A novel comprehensive experimental study concerned graphene oxide nanoparticles dispersed in water: Synthesise, characterisation, thermal conductivity measurement and present a new approach of RLSF neural network. *International Communications in Heat and Mass Transfer*, *109*(5), 104333. https://doi.org/10.1016/j.icheatmasstransfer.2019.104333

Ma, Y., Jafari, M., Barzinjy, A. A., Mahmoudi, B., Hamad, S. M., & Afrand, M. (2020). The effect of inlet temperature on the irreversibility characteristics of non-Newtonian hybrid nano-fluid flow inside a minichannel counter-current hairpin heat exchanger. *Journal of Thermal Analysis and Calorimetry*, *139*(6), 3789–3801. https://doi.org/10.1007/s10973-019-08671-1

Malekahmadi, O., Kalantar, M., & Nouri-Khezrabad, M. (2021). Effect of carbon nanotubes on the thermal conductivity enhancement of synthesized hydroxyapatite filled with water for dental applications: Experimental characterization and numerical study. *Journal of Thermal Analysis and Calorimetry*, *144*(6), 2109–2126. https://doi.org/10.1007/s10973-021-10593-w

Maleki, A., Elahi, M., Assad, M. E. H., Alhuyi Nazari, M., Safdari Shadloo, M., & Nabipour, N. (2021). Thermal conductivity modeling of nanofluids with ZnO particles by using approaches based on artificial neural network and MARS. *Journal of Thermal Analysis and Calorimetry*, *143*(6), 4261–4272. https://doi.org/10.1007/s10973-020-09373-9

Moosavi, S. R., Wood, D. A., Ahmadi, M. A., & Choubineh, A. (2019). ANN-based prediction of laboratory-scale performance of CO_2-foam flooding for improving oil recovery. *Natural Resources Research*, *28*(4), 1619–1637. https://doi.org/10.1007/s11053-019-09459-8

Nguyen, Q., Ghorbani, P., Bagherzadeh, S. A., Malekahmadi, O., & Karimipour, A. (2020). Performance of joined artificial neural network and genetic algorithm to study the effect of temperature and mass fraction of nanoparticles dispersed in ethanol. *Mathematical Methods in the Applied Sciences 77*, ((11), 188–198. https://doi.org/10.1002/mma.6688.

Nguyen, Q., Rizvandi, R., Karimipour, A., Malekahmadi, O., & Bach, Q. V. (2020). A novel correlation to calculate thermal conductivity of aqueous hybrid graphene oxide/silicon dioxide nanofluid: Synthesis, characterizations, preparation, and artificial neural network modeling. *Arabian Journal for Science and Engineering*, *45*(11), 9747–9758. https://doi.org/10.1007/s13369-020-04885-w

Rahmat, A., Barigou, M., & Alexiadis, A. (2019). Numerical simulation of dissolution of solid particles in fluid flow using the SPH method. *International Journal of Numerical Methods for Heat & Fluid Flow*, 654–670. https://doi.org/10.1108/HFF-05-2019-0437

Rahmat, A., Tofighi, N., & Yildiz, M. (2017). The combined effect of electric forces and confinement ratio on the bubble rising. *International Journal of Heat and Fluid Flow*, *65*, 352–362. https://doi.org/10.1016/j.ijheatfluidflow.2017.01.002

Rajpal, N. (2014, February). Comparative analysis of feed forward and radial basis function neural networks for the reconstruction of noisy curves. In *2014 International Conference on Reliability Optimization and Information Technology (ICROIT)* (pp. 353–358). IEEE. https://doi.org/10.1109/ICROIT.2014.6798353.

Ranjbarzadeh, R., Akhgar, A., Musivand, S., & Afrand, M. (2018). Effects of graphene oxide–silicon oxide hybrid nanomaterials on rheological behavior of water at various time durations and temperatures: Synthesis, preparation and stability. *Powder Technology*, *335*(7), 375–387. https://doi.org/10.1016/j.powtec.2018.05.036

Ranjbarzadeh, R., Karimipour, A., Afrand, M., Isfahani, A. H. M., & Shirneshan, A. (2017). Empirical analysis of heat transfer and friction factor of water/graphene oxide nanofluid flow in turbulent regime through an isothermal pipe. *Applied Thermal Engineering*, *126*(5), 538–547. https://doi.org/10.1016/j.applthermaleng.2017.07.189

Ranjbarzadeh, R., Moradikazerouni, A., Bakhtiari, R., Asadi, A., & Afrand, M. (2019). An experimental study on stability and thermal conductivity of water/silica nanofluid: Eco-friendly production of nanoparticles. *Journal of Cleaner Production*, *206*(4), 1089–1100. https://doi.org/10.1016/j.jclepro.2018.09.205

Safaei, M. R., Ranjbarzadeh, R., Hajizadeh, A., Bahiraei, M., Afrand, M., & Karimipour, A. (2019). Effects of cobalt ferrite coated with silica nanocomposite on the thermal conductivity of an antifreeze: New nanofluid for refrigeration condensers. *International Journal of Refrigeration*, *102*(8), 86–95. https://doi.org/10.1016/j.ijrefrig.2018.12.007

Santos, R., Rupp, M., Bonzi, S., & Fileti, A. M. (2013). Comparison between multilayer feedforward neural networks and a radial basis function network to detect and locate leaks in pipelines transporting gas. *Chemical Engineering Transactions*, *32*(9), 1375–1380. https://doi.org/10.3303/CET1332230

Sedeh, R. N., Abdollahi, A., & Karimipour, A. (2019). Experimental investigation toward obtaining nanoparticles' surficial interaction with basefluid components based on measuring thermal conductivity of nanofluids. *International Communications in Heat and Mass Transfer*, *103*, 72–82. https://doi.org/10.1016/j.icheatmasstransfer.2019.02.01610

Shafiei, A., Ahmadi, M. A., Zaheri, S. H., Baghban, A., Amirfakhrian, A., & Soleimani, R. (2014). Estimating hydrogen sulfide solubility in ionic liquids using a machine learning approach. *The Journal of Supercritical Fluids*, *95*(16), 525–534. https://doi.org/10.1016/j.supflu.2014.08.011

Sun, C., Taherifar, S., Malekahmadi, O., Karimipour, A., Karimipour, A., & Bach, Q. V. (2021). Liquid paraffin thermal conductivity with additives tungsten trioxide nanoparticles: Synthesis and propose a new composed approach of fuzzy logic/artificial neural network. *Arabian Journal for Science and Engineering*, *46*(3), 2543–2552. https://doi.org/10.1007/s13369-020-05151-9

Teng, T. P., Hung, Y. H., Teng, T. C., Mo, H. E., & Hsu, H. G. (2010). The effect of alumina/water nanofluid particle size on thermal conductivity. *Applied Thermal Engineering*, *30*(14–15), 2213–2218. https://doi.org/10.1016/j.applthermaleng.2010.05.036

Wang, N., Maleki, A., Alhuyi Nazari, M., Tlili, I., & Safdari Shadloo, M. (2020). Thermal conductivity modeling of nanofluids contain MgO particles by employing different approaches. *Symmetry*, *12*(2), 206. https://doi.org/10.3390/sym12020206

Xu, Y., Nguyen, Q., Malekahmadi, O., Hadi, R., Jokar, Z., Mardani, A., & Bach, Q. V. (2020). Synthesis and characterization of additive graphene oxide nanoparticles dispersed in water: Experimental and theoretical viscosity prediction of non-Newtonian nanofluid. *Mathematical Methods in the Applied Sciences 11*, ((5), 324–344. https://doi.org/10.1002/mma.6381.

Zheng, Y., Shadloo, M. S., Nasiri, H., Maleki, A., Karimipour, A., & Tlili, I. (2020). Prediction of viscosity of biodiesel blends using various artificial model and comparison with empirical correlations. *Renewable Energy*, *153*(5), 1296–1306. https://doi.org/10.1016/j.renene.2020.02.087